STANDARD ARTICLE

Journal of Veterinary Internal Medicine ACVIM
Open Access
American College of Veterinary Internal Medicine

Brain perfusion magnetic resonance imaging using pseudocontinuous arterial spin labeling in 314 dogs and cats

Anne-Cécile Hoffmann[1] | Yannick Ruel[1] | Kirsten Gnirs[2] | Stella Papageorgiou[2] | Luca Zilberstein[3] | Sarah Nahmani[4] | Nathalie Boddaert[4,5] | Hugues Gaillot[1]

[1]Unit of Diagnostic Imaging, ADVETIA Veterinary Referral Hospital, Vélizy-Villacoublay, France

[2]Unit of Neurology, ADVETIA Veterinary Referral Hospital, Vélizy-Villacoublay, France

[3]Unit of Anesthesiology-Analgesia, ADVETIA Veterinary Referral Hospital, Vélizy-Villacoublay, France

[4]Paediatric Radiology Department, AP-HP, Hôpital Necker Enfants Malades, Université de Paris, Paris, France

[5]Universié de Paris, Institut Imagine INSERM U1163, Paris, France

Correspondence
Hugues Gaillot, Unit of Diagnostic Imaging, ADVETIA Veterinary Referral Hospital, 9 avenue Louis Bréguet, 78 140 Vélizy-Villacoublay, France.
Email: gaillot@advetia.fr

Abstract

Background: Arterial spin labeling (ASL) is a noninvasive brain perfusion magnetic resonance imaging (MRI) technique that has not been assessed in clinical veterinary medicine.

Hypothesis/Objectives: To test the feasibility of ASL using a 1.5 Tesla scanner and provide recommendations for optimal quantification of cerebral blood flow (CBF) in dogs and cats.

Animals: Three hundred fourteen prospectively selected client-owned dogs and cats.

Methods: Each animal underwent brain MRI including morphological sequences and ≥1 ASL sequences using different sites of blood labeling and postlabeling delays (PLD). Calculated ASL success rates were compared. The CBF was quantified in animals that had morphologically normal brain MRI results and parameters of ASL optimization were investigated.

Results: Arterial spin labeling was easily implemented with an overall success rate of 95% in animals with normal brain MRI. Technical recommendations included (a) positioning of the imaging slab at the foramen magnum and (b) selected PLD of 1025 ms in cats and dogs <7 kg, 1525 ms in dogs 7 to 38 kg, and 2025 ms in dogs >38 kg. In 37 dogs, median optimal CBF in the cortex and thalamic nuclei were 114 and 95 mL/100 g/min, respectively. In 28 cats, median CBF in the cortex and thalamic nuclei were 113 and 114 mL/100 g/min, respectively.

Conclusions and Clinical Importance: Our survey of brain perfusion ASL-MRI demonstrated the feasibility of ASL at 1.5 Tesla, suggested technical recommendations and provided CBF values that should be helpful in the characterization of various brain diseases in dogs and cats.

KEYWORDS
arterial spin labeling, ASL, brain, cat, dog, MRI, perfusion

2328 | **Journal of Veterinary Internal Medicine** ACVIM
Open Access
American College of
Veterinary Internal Medicine

HOFFMANN ET AL.

1 | INTRODUCTION

Measurement of brain perfusion has become an indispensable tool in the clinical evaluation of brain disorders in humans including strokes, cerebrovascular malformations, tumors, epilepsy, encephalitis, and degenerative diseases.[1-8] Several techniques have been developed to evaluate brain perfusion based on computed tomography (CT), magnetic resonance imaging (MRI), and nuclear medicine.[9,10] The major limitations of these techniques are IV injection of an exogenous contrast agent and, with CT and nuclear medicine techniques, exposure to ionizing radiation. Since the early 1990s, a noninvasive MRI technique to assess brain perfusion has emerged first in neurosciences research and then in clinical neuroimaging: arterial spin labeling (ASL).[2-4,11-28] Arterial spin labeling uses arterial blood water as a freely diffusible endogenous flow tracer. Blood water entering the brain is labeled by magnetic inversion and, after a postlabeling delay (PLD), a labeled image of the brain is acquired. The perfusion signal is obtained by subtracting the labeled image from a control image in which blood has not been labeled, resulting in an image with the signal intensity proportional to cerebral blood flow (CBF).[14,29] The technique of ASL-MRI provides an absolute and quantitative voxel-by-voxel measurement of resting CBF without any agent injection, and without any exposure to ionizing radiation,[8,30] thus offering new opportunities to quantify CBF at rest in humans. The CBF quantified using ASL-MRI is expressed as a volume of blood per volume of tissue per minute (mL/100 g/min).[14,31]

In animals, brain ASL-MRI has been used widely in experimental research.[2-5,12] In veterinary medicine, few publications have dealt with cerebral perfusion MRI, most of them describing dynamic studies that rely on IV injection of a gadolinium-based contrast agent.[32-35] To our knowledge, veterinary clinical application of ASL brain perfusion MRI has only been mentioned in 2 publications.[36,37] It was first introduced in veterinary medicine as a technique providing a weak MRI signal that can be influenced by several technical factors.[36] One year later, an ASL protocol was implemented in a dog with suspected late subacute cortical laminar necrosis using a 3 Tesla MRI scanner.[37]

Considering the broad clinical application of ASL perfusion imaging in humans and particularly in children, we hypothesized that ASL would be clinically useful in the diagnosis of various neurological disorders in dogs and cats. We hypothesized that ASL performed at 1.5 Tesla would effectively and efficiently assess brain perfusion, and that CBF could be measured using ASL-MRI in both species. Our aims were (a) to test the feasibility of ASL-MRI at 1.5 Tesla for assessing brain perfusion and (b) to provide settings and specific recommendations for optimal quantification of CBF in dogs and cats using ASL.

2 | MATERIALS AND METHODS

2.1 | Study design and timing

This study consisted of a single-center (ADVETIA Veterinary Referral Hospital), prospective, observational design, approved by the Ethics Committee Jacques Bonnod of VetAgro Sup and performed with informed owner consent. The study had a fixed time frame of 16 months (March 2018 to June 2019) and was divided into 3 equal periods of time corresponding to 3 different phases that were conducted sequentially.

All cats and dogs were selected by 2 board-certified veterinary neurologists (Diplomates of the European College of Veterinary Neurology). To be included, animals had to have a recommendation for brain MRI by a neurologist and be free of any contraindication to general anesthesia.

2.2 | Anesthesia

Premedication protocol was based on the patient's physical status and using dexmedetomidine, butorphanol, midazolam, or some combination of these drugs. In all animals, general anesthesia was induced with propofol and maintained with isoflurane diluted in oxygen. During the procedure, respiratory carbon dioxide concentration (ETCO$_2$), respiratory rate, and arterial pulse rate were recorded continuously.

2.3 | Magnetic resonance imaging

Magnetic resonance images were obtained using a 1.5 T MR unit (Signa Explorer SV25; GE Medical Systems, Milwaukee, Wisconsin) with a 16-channel flex coil. The brain imaging protocol included all standard brain imaging pulse sequences used at our institution: 3D T1, 3D fluid-attenuated inversion recovery, 2D or 3D T2, 3D T2*, diffusion, and gadolinium-enhanced 3D T1. Detailed information about these sequences is provided in Supporting Information 1. Additionally, each MRI study included ≥1 3D pseudocontinuous ASL perfusion imaging pulse sequences that were acquired in a transverse plane before IV injection of gadolinium. The ASL sequence settings are provided in Supporting Information 2. Patients were positioned in sternal recumbency. The arterial spin tagging plane was parallel to the transverse plane of the neck and was automatically set 2 cm caudal to the caudal border of the imaging slab. The imaging slab positioning (ie, the site of blood tagging) and the PLD value varied according to the phase of the study and are summarized in Table 1. During phase 1, the caudal border of the imaging slab was placed over the mid-length of the second cervical vertebra (mid-C2 position) and the PLD was set at 1025 ms. Animals enrolled during phase 1 formed the group called "group mid-C2." During phase 2, the caudal border of the imaging slab was placed just caudal to the cerebellum (foramen magnum [FM] position), and the PLD was kept at 1025 ms. During phase 3, the caudal border of the imaging slab was placed just caudal to the cerebellum (FM position) and 3 ASL sequences set at 3 different PLDs (1025, 1525, and 2025 ms) were performed on each animal. Animals enrolled during phases 2 and 3 formed the group called "group FM." The MR images were stored in a picture archiving communication system (PACS) and analyzed by using a dedicated medical image viewer (Vue PACS, version 12.1.6; Philips, Amsterdam, the Netherlands).

2.4 | Quality patterns of ASL studies and acronyms

The following acronyms were used for depicting different quality patterns of ASL studies: "gASL" for good diagnostic quality and "pASL" for poor diagnostic quality (failed ASL), the latter including "pASL-B" (B for bilateral), "pASL-U(hemi)" (U(hemi) for unilateral-hemiencephalon), and "pASL-U(pro)" (U(pro) for unilateral-prosencephalon). Table 2 details the descriptive criteria and shows a CBF color map example for each ASL pattern. Recommendations used for ASL acronym assignment are provided in Supporting Information 3. Figure 1 provides a detailed anatomical comparison between gASL images and T2-weighted images.

2.5 | Data collection

Signalment (breed, sex, age, and weight), premedication and anesthesia protocols (drugs used for premedication, induction and maintenance of general anesthesia), monitored physiological parameters (pulse rate, respiratory rate and $ETCO_2$ during ASL image acquisition), and final or presumed diagnosis were recorded from medical records. Brain MRI was classified as either normal or pathological; criteria used to determine "normal brain MRI" are provided in Supporting Information 4.

TABLE 1 Arterial spin labeling pulse sequence parameters distinguishing the three phases of the study

| Phase of the study	Phase 1	Phase 2	Phase 3
Imaging slab positioning	mid-C2	FM	FM
PLD selected	1025 ms	1025 ms	1025 ms 1525 ms 2025 ms

Note: See text for a detailed description of imaging slab positioning. Abbreviations: FM, foramen magnum; mid-C2, mid-length of the second cervical vertebra; PLD, postlabeling delay.

TABLE 2 Acronyms, descriptive criteria, and examples of CBF color map of ASL quality patterns

Acronym	Descriptive criteria	CBF color map
gASL	Symmetrical brain perfusion signal allowing discrimination of: ° regions with high signal intensity: cerebral cortex, central gray nuclei, cerebellar cortex and vermis ° regions with intermediate signal intensity: brain white matter ° regions with no perfusion signal: ventricles	
pASL-B	Bilateral lack of perfusion signal in both the right and left prosencephalon. Perfusion signal is variably present in other brain regions	
pASL-U(hemi)	Unilateral lack of perfusion signal limited to one hemiencephalon (right or left)	
pASL-U(pro)	Unilateral lack of perfusion signal limited to one prosencephalon (right or left)	
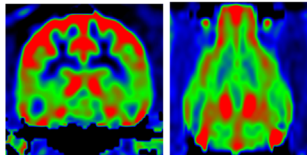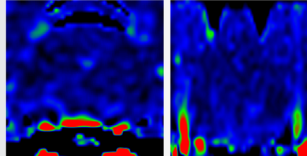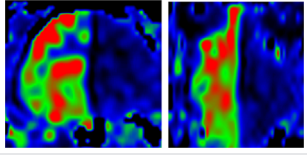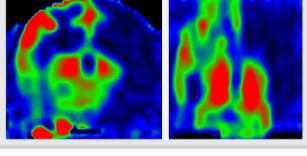
Notes: Transverse (A, C, E, G) and dorsal (B, D, F, H) reconstructed CBF color maps with image planes crossing the interthalamic adhesion, in 3 dogs (A, B, C, D, G, H) and a cat (E, F). (A) and (B): gASL pattern in a 1.5-year-old male intact Portuguese Sheepdog diagnosed with idiopathic facial nerve paralysis. A symmetrical high signal intensity (red) is noticed in the cerebral cortex and the thalamic nuclei. A symmetrical intermediate signal intensity (green) is noticed in the cerebral white matter. (C) and (D): pASL-B pattern in an 8-year-old male intact Shepherd dog diagnosed with a left-sided idiopathic Horner's syndrome. Bilateral absence of brain perfusion signal. Branches of the right and the left external carotid arteries show an elevated signal intensity (red).
(E) and (F): pASL-U(hemi) pattern in a 16-year-old female spayed cat with suspected age-related behavioral changes. Unilateral (left-sided) absence of perfusion signal in the cerebral arterial territory of the left external carotid artery (maxillary branch) in cats (left hemiencephalon). (G) and (H): pASL-U(pro) pattern in a 3.5-year-old Chihuahua diagnosed with a necrotizing cerebellitis. Unilateral (left-sided) absence of perfusion signal in the cerebral arterial territory of the left internal carotid artery in dogs (left prosencephalon).
Abbreviations: gASL, good diagnostic quality ASL study; pASL-B, poor diagnostic quality ASL study with bilateral lack of signal; pASL-U(hemi), poor diagnostic quality ASL study with unilateral lack of signal in one hemiencephalon (right or left); pASL-U(pro), poor diagnostic quality ASL study with unilateral lack of signal in one prosencephalon (right or left).
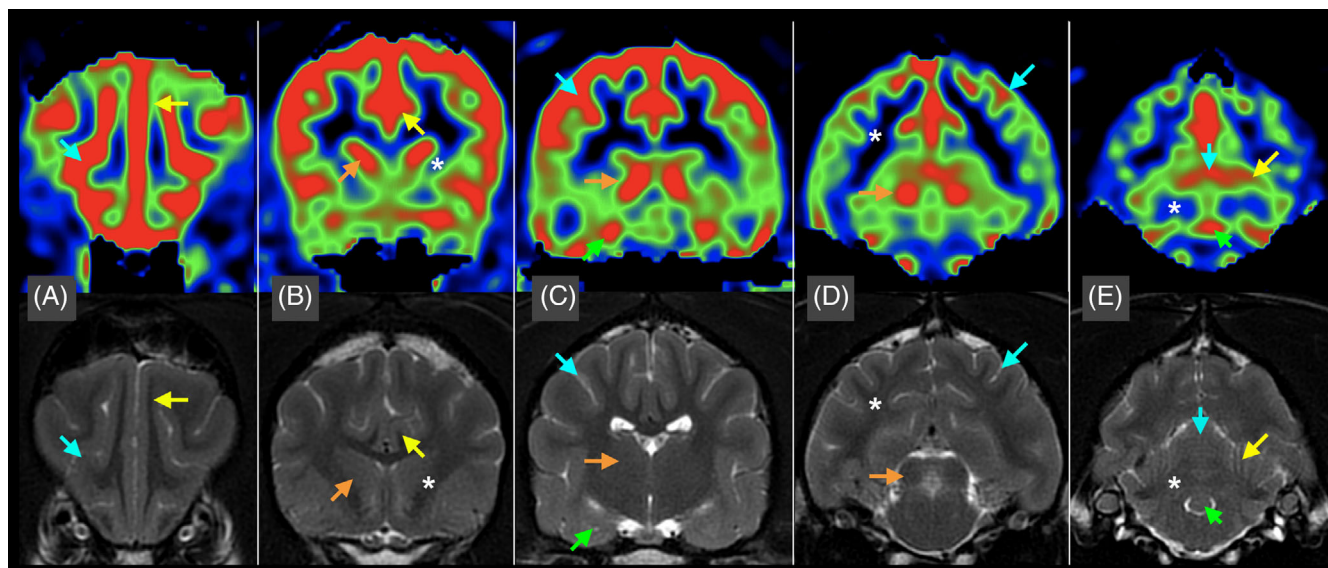
FIGURE 1 Good diagnostic quality brain ASL perfusion images (gASL pattern) and corresponding anatomical MR images in a dog. A 1.5-year-old male intact Portuguese Sheepdog diagnosed with idiopathic facial nerve paralysis. Top row shows arterial spin labeling (ASL) cerebral blood flow (CBF) color map transverse images. Highly perfused anatomical structures are depicted in red, moderately perfused structures are depicted in green, and poorly to not perfused structures are depicted in dark blue to black. Bottom row shows corresponding T2-weighted transverse images obtained at the same anatomic levels as ASL images. A, Frontal lobes level: presylvian groove (blue arrow), cingulate gyrus (yellow arrow). B, Parietal lobes level: cingulate gyrus (yellow arrow) and caudate nucleus (orange arrow), and internal capsule (white asterisk). C, Thalamus level: middle suprasylvian groove (blue arrow), thalamic nucleus (orange arrow), and piriform lobe and parahippocampal gyrus (green arrow). D, Mesencephalon level: mesencephalic nucleus (orange arrow), marginal groove (blue arrow), and corona radiata (white asterisk). E, Cerebellum level: cerebellar vermis (blue arrows), cerebellar cortex (yellow arrow), lingula of cerebellum (green arrow), and cerebellar white matter (white asterisk)

A board-certified veterinary radiologist (Diplomate of the European College of Veterinary Diagnostic Imaging [ECVDI]) with 1 year of ASL experience gained in human pediatric neuroimaging (H. Gaillot) and a second-year radiology resident (A.-C. Hoffmann) reviewed all ASL studies as primary readers for assigning a quality pattern acronym by consensus. Any ASL images with questionable diagnostic quality were further reviewed and assigned by consensus using a third primary reader, a neuroradiologist with 20 years of experience in human pediatric neuroimaging (N. Boddaert).

Another investigator, a board-certified veterinary radiologist with no experience in ASL (Y. Ruel), assessed ASL image quality in all animals in phase 3, as a secondary reader for the purpose of measuring inter-reader reliability.

The presence or absence of signal in the branches of each external carotid artery (ECA) also was recorded. The ASL success rate (ASL-SR) was calculated as the percentage of ASL studies with good diagnostic quality.

Cerebral blood flow was quantified in the cerebral cortex (exclusively cortical gray matter) and thalamic nuclei on transverse brain images crossing the interthalamic adhesion by drawing 2 round 2-dimensional regions of interest (ROI; surface area: 6-12 mm^2), 1 in the most densely perfused area of the cortex (middle suprasylvian groove), and 1 in the most densely perfused area of the ipsilateral thalamus (thalamic nuclei).

2.6 | Radiographic detection of an identification microchip

In group FM animals, the presence of a cervical microchip was investigated radiographically. The chip location relative to the spine was recorded, and the chip-to-FM distance was measured on a dorsoventral view.

In group FM, pASL-U animals were compared with gASL animals considering only PLD of 1025 ms. Association of pASL-U group and gASL group with the absence of signal in the ECA branches was calculated. Monovariate and multivariate analyses were performed on the following variables: sex ratio, age, pulse rate, presence of a cervical chip with a left lateral or left ventrolateral location, a chip-to-FM distance <4 cm, body weight <6.5 kg, and a chip-to-FM distance >6 cm.

2.7 | Positioning of the imaging slab

The impact of imaging slab positioning on ASL quality was assessed by comparing group mid-C2 animals with group FM animals considering only PLD of 1025 ms. For each group, monovariate and multivariate analyses were performed on the following variables: age, weight, sex ratio, dog/cat distribution, ETCO$_2$, use of dexmedetomidine, pulse rate, and presence of a lesion on standard brain MRI.

2.8 | Cerebral blood flow measurement

In group FM cats with normal brain MRI and gASL pattern, CBF was quantified in the cerebral cortex and the thalamic nuclei on ASL images obtained using a PLD of 1025 ms.

In phase 3 dogs with normal brain MRI and gASL pattern with at least 1 PLD, CBF was quantified in the cerebral cortex and the thalamic nuclei on gASL images obtained using any PLD (1025, 1525, or 2025 ms).

2.9 | Optimal PLD

For each gASL dog in phase 3, "optimal PLD" was defined as the PLD providing the highest cortical CBF value. In dogs with normal brain MRI, cortical and thalamic CBF values obtained using the optimal PLD were referred as "optimal cortical CBF" and "optimal thalamic CBF."

2.10 | Statistical analysis

Data were analyzed by 1 of the investigators (S. Nahmani) using R Core Team (2020) language and environment for statistical computing (R Foundation for Statistical Computing, Vienna, Austria. URL https://www.R-project.rog/). Inter-reader agreement was measured by calculating Cohen's kappa coefficient. Data were assessed for normality using the Shapiro-Wilk test. Continuous data were expressed as medians, interquartile range (IQR) and ranges, or mean and standard deviation if normally distributed. Categorical data were expressed as frequencies and percentages. Comparisons of categorical data between groups were performed using Chi-squared test with Yates's continuity correction or Fisher exact test for smaller sample sizes. Comparisons of continuous data between groups were made using Mann-Whitney test, Student t test for normally distributed data or Wilcoxon signed-ranked test for matched groups. Multivariate analyses using logistic regression were performed to identify (a) factors that could significantly influence the occurrence of a pASL-U pattern such as a cervical chip, (b) factors that could significantly influence ASL-SR such as slab position, (c) association of different ranges of weight (<7 kg; 6-39 kg; >38 kg) with a particular optimal PLD in

dogs, and (d) factors that could be significantly associated with ASL failure despite proper slab position and optimal PLD. Magnitude and uncertainty of effects were assessed by calculating odds ratios (ORs) and 95% confidence intervals (95% CIs). Significance was set at $P < .05$.

3 | RESULTS

3.1 | Study population

Three-hundred and fourteen animals (248 dogs and 66 cats) were included. Age, weight, and sex ratio in dogs and cats according to the phase of the study are presented in Table 3. The 16 most frequently represented dog breeds (≥5 dogs per breed) corresponding to 163 dogs are listed in Supplemental Table 1 provided in Supporting Information 5.

3.2 | Flowcharts of the study and overall ASL-SR for each phase

Two flowcharts of the study are provided in Figure 2. The distribution of animals according to ASL pattern, species, normal or pathological brain MRI results, and corresponding ASL-SRs are presented for each phase of the study in Tables 4 to 8.

In dogs, the highest ASL-SR was obtained using a PLD of 1525 ms and FM position of the slab, in both normal and pathological brain MRI groups, and was 97.4% (37/38) and 81.8% (27/33), respectively (Table 7).

In cats, a relevant ASL-SR only could be provided using a PLD of 1025 ms and FM position of the slab, in both normal and pathological brain MRI groups, and was 96.6% (28/29) and 80% (8/10), respectively (Tables 5 and 6).

3.3 | Inter-reader agreement

Agreement between primary and secondary readers was observed in 86/87 animals in phase 3. Cohen's kappa coefficient evaluating agreement between secondary and primary readers was 0.96, indicating excellent reliability between readers.

TABLE 3 Age, body weight, and sex ratio in dogs and cats in each phase of the study

	Phase 1	Phase 2	Phase 3
Dogs (n = 248)	(n = 78)	(n = 96)	(n = 74)
Age (mean ± SD; years)	7.5 ± 4.2	7.5 ± 4.2	7.4 ± 4.0
Weight (mean ± SD; kg)	19.5 ± 16.2	15.2 ± 10.8	17.2 ± 12.2
Sex ratio (M/F)	1.69 (49/29)	0.78 (42/54)	0.95 (36/38)
Cats (n = 66)	(n = 16)	(n = 37)	(n = 13)
Age (mean ± SD; years)	7.7 ± 4.5	9.0 ± 4.5	8.4 ± 5.4
Weight (mean ± SD; kg)	4.2 ± 0.7	4.5 ± 1.4	4.4 ± 1.1
Sex ratio (M/F)	1.29 (9/7)	1.64 (23/14)	0.86 (6/7)

Dogs and cats in the global study
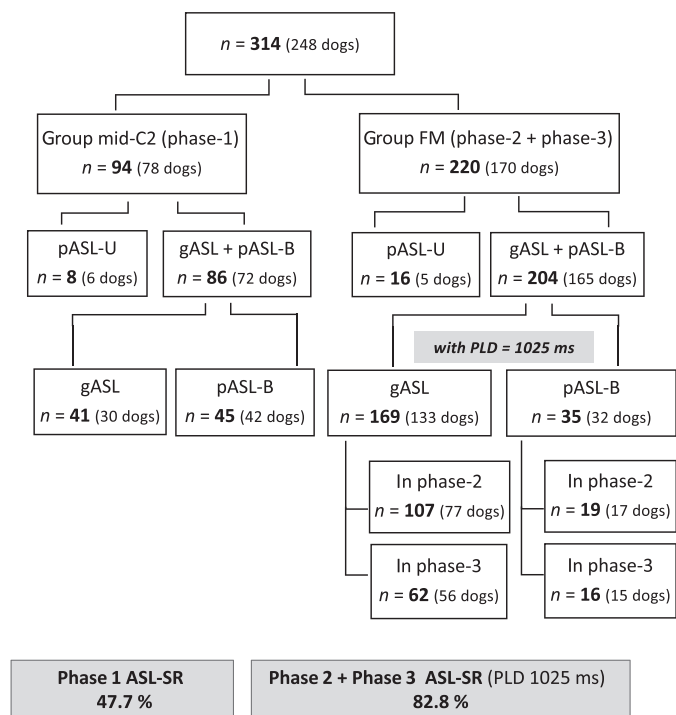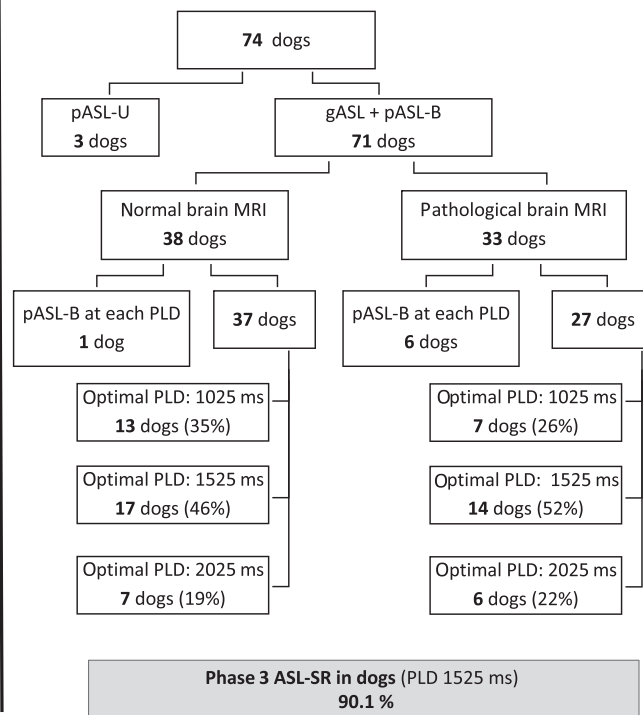

Dogs in phase 3

FIGURE 2   Flow chart of the entire study and flow chart of phase 3 of the study. Group mid-C2: animals enrolled during phase 1 (slab positioned over the mid-length of the second cervical vertebra). Group foramen magnum (FM): animals enrolled during phases 2 and 3 (slab positioned over the foramen magnum). pASL-U: arterial spin labeling (ASL) pattern indicating a unilateral lack of brain perfusion signal (poor diagnostic quality ASL study). gASL: ASL pattern indicating a good diagnostic quality ASL study. pASL-B: ASL pattern indicating a bilateral lack of brain perfusion signal (poor diagnostic quality ASL study). Optimal postlabeling delay (PLD): PLD value (1025, 1525, or 2025 ms) that provided, for a given dog in phase 3, a gASL pattern and the highest value of cerebral blood flow measured in the prosencephalic cortex. Phase 1: slab at mid-C2 and PLD set at 1025 ms; Phase 2: slab at FM and PLD set at 1025 ms; Phase 3: slab at FM and PLD set at three different values (1025, 1525, and 2025 ms). n, number of animals (dogs and cats)

TABLE 4   Distribution of animals in phase 1 (n = 94) according to ASL patterns, species (dogs or cats) and brain MRI results (normal or pathological MRI), and corresponding ASL-SR

| | Phase 1 (slab at mid-C2; PLD 1025 ms) | | | | |
	Total	gASL	pASL-U	pASL-B	ASL-SR
All animals	94	41	8	45	47.7%
Normal MRI	56/94	22	7	27	44.9%
Pathological MRI	38/94	19	1	18	51.4%
Dogs	78	30	6	42	41.7%
Normal MRI	45/78	15	5	25	37.5%
Pathological MRI	33/78	15	1	17	46.9%
Cats	16	11	2	3	78.6%
Normal MRI	11/16	7	2	2	77.8%
Pathological MRI	5/16	4	0	1	80%

Note: The ASL-SRs have been calculated, after excluding animals with pASL-U pattern (see text for explanation), as follows: $100 \times gASL/(gASL + pASL-B)$.
Abbreviations: ASL-SR, ASL success rate; gASL, good diagnostic quality ASL study; mid-C2, mid-length of the second cervical vertebra; pASL-B, poor diagnostic quality ASL study with bilateral lack of signal; pASL-U, poor diagnostic quality ASL study with unilateral lack of signal; PLD, postlabeling delay.

TABLE 5 Distribution of animals in phase 2 (n = 133) according to ASL pattern, species (dog or cat) and brain MRI result (normal or pathological MRI), and corresponding ASL-SR

	Phase 2 (slab at FM; PLD 1025 ms)				
	Total	gASL	pASL-U	pASL-B	ASL-SR
All animals	133	107	7	19	84.9%
Normal MRI	81/133	67	4	10	87%
Pathological MRI	52/133	40	3	9	81.6%
Dogs	96	77	2	17	81.9%
Normal MRI	54/96	44	0	10	81.5%
Pathological MRI	42/96	33	2	7	82.5%
Cats	37	30	5	2	93.8%
Normal MRI	27/37	23	4	0	100%
Pathological MRI	10/37	7	1	2	77.8%

Note: The ASL-SRs have been calculated, after excluding animals with pASL-U pattern (see text for explanation), as follows: $100 \times$ gASL/(gASL + pASL-B).

Abbreviations: ASL-SR, ASL success rate; FM, foramen magnum; gASL, good diagnostic quality ASL study; pASL-B, poor diagnostic quality ASL study with bilateral lack of signal; pASL-U, poor diagnostic quality ASL study with unilateral lack of signal; PLD, postlabeling delay.

TABLE 6 Distribution of animals in phase 3 (n = 87) with PLD set at 1025 ms according to ASL pattern, species (dog or cat) and brain MRI result (normal or pathological MRI), and corresponding ASL-SR

	Phase 3 (slab at FM; PLD 1025 ms)				
	Total	gASL	pASL-U	pASL-B	ASL-SR
All animals	87	62	9	16	79.5%
Normal MRI	49/87	39	5	5	88.6%
Pathological MRI	38/87	23	4	11	67.6%
Dogs	74	56	3	15	78.9%
Normal MRI	39/74	34	1	4	89.5%
Pathological MRI	35/74	22	2	11	66.7%
Cats	13	6	6	1	85.7%[a]
Normal MRI	10/13	5	4	1	83.3%[a]
Pathological MRI	3/13	1	2	0	100%[a]

Note: The ASL-SRs have been calculated, after excluding animals with pASL-U pattern (see text for explanation), as follows: $100 \times$ gASL/(gASL + pASL-B).

Abbreviations: ASL-SR, ASL success rate; FM, foramen magnum; gASL, good diagnostic quality ASL study; pASL-B, poor diagnostic quality ASL study with bilateral lack of signal; pASL-U, poor diagnostic quality ASL study with unilateral lack of signal; PLD, postlabeling delay.

[a]Results considered irrelevant considering the small number of cats being enrolled.

3.4 | Unilateral lack of brain perfusion signal: pASL-U pattern

A pASL-U pattern was observed in 24/314 animals (7.6%) and in each phase of the study.

In group FM, results of comparison of pASL-U animals (n = 16) with gASL animals (n = 169) are presented in Supplemental Table 2, provided in Supporting Information 6. These findings indicate that a lateral/ventrolateral cervical microchip close to the FM induced an ipsilateral unilateral failure of ASL. Consequently, in the following results, all pASL-U animals have been excluded because this pattern was considered to be artefactual, leading to a resized population studied (phase 1, n = 86; phase 2, n = 126; phase 3, n = 78).

3.5 | Positioning of the imaging slab

The impact of imaging slab position on ASL image quality was assessed using univariate analysis by comparing group mid-C2 animals with group FM animals after excluding pASL-U cases. Results are presented in Supplemental Table 3 provided in Supporting Information 7. The ASL-SR was significantly higher in group FM (82.8%, 169/204) than in group mid-C2 (47.7%, 41/86; $P < .001$). Group FM was 5.12 times more likely to have good diagnostic quality ASL than group mid-C2 (OR, 5.12; 95% CI, 2.94-8.93; $P < .001$). In the population studied above, gASL animals and pASL-B animals were compared for slab positioning and other variables using multivariate analysis. Results are presented in Supplemental Table 4 provided in Supporting Information 8 and showed that FM position of the slab was significantly more frequent in gASL animals (80%, 169/210) than

	Phase 3 (slab at FM; PLD 1525 ms)				
	Total	gASL	pASL-U	pASL-B	ASL-SR
All animals	87	71	9	7	91%
Normal MRI	49/87	43	5	1	97.7%
Pathological MRI	38/87	28	4	6	82.4%
Dogs	74	64	3	7	90.1%
Normal MRI	39/74	37	1	1	97.4%
Pathological MRI	35/74	27	2	6	81.8%
Cats	13	7	6	0	100%[a]
Normal MRI	10/13	6	4	0	100%[a]
Pathological MRI	3/13	1	2	0	100%[a]

TABLE 7 Distribution of animals in phase 3 (n = 87) with PLD set at 1525 ms according to ASL pattern, species (dog or cat) and brain MRI result (normal or pathological MRI), and corresponding ASL-SR

Note: The ASL-SRs have been calculated, after excluding animals with pASL-U pattern (see text for explanation), as follows: $100 \times gASL/(gASL + pASL\text{-}B)$.
Abbreviations: ASL-SR, ASL success rate; FM, foramen magnum; gASL, good diagnostic quality ASL study; pASL-B, poor diagnostic quality ASL study with bilateral lack of signal; pASL-U, poor diagnostic quality ASL study with unilateral lack of signal; PLD, postlabeling delay.
[a]Results considered irrelevant considering the small number of cats being enrolled.

	Phase 3 (slab at FM; PLD 2025 ms)				
	Total	gASL	pASL-U	pASL-B	ASL-SR
All animals	87	70	9	8	89.7%
Normal MRI	49/87	42	5	2	95.5%
Pathological MRI	38/87	28	4	6	82.4%
Dogs	74	63	3	8	88.7%
Normal MRI	39/74	36	1	2	94.7%
Pathological MRI	35/74	27	2	6	81.8%
Cats	13	7	6	0	100%[a]
Normal MRI	10/13	6	4	0	100%[a]
Pathological MRI	3/13	1	2	0	100%[a]

TABLE 8 Distribution of animals in phase 3 (n = 87) with PLD set at 2025 ms according to ASL pattern, species (dog or cat) and brain MRI result (normal versus pathological MRI), and corresponding ASL-SR

Note: The ASL-SRs have been calculated, after excluding animals with pASL-U pattern (see text for explanation), as follows: $100 \times gASL/(gASL + pASL\text{-}B)$.
Abbreviations: ASL-SR, ASL success rate; FM, foramen magnum; gASL, good diagnostic quality ASL study; pASL-B, poor diagnostic quality ASL study with bilateral lack of signal; pASL-U, poor diagnostic quality ASL study with unilateral lack of signal; PLD, postlabeling delay.
[a]Results considered irrelevant considering the small number of cats being enrolled.

in pASL-B animals (43.8%, 35/80; OR, 1.46; 95% CI, 1.30-1.64; $P < .001$). No significant difference was found between the 2 groups in sex ratio (OR, 1.00; 95% CI, 0.91-1.11; $P = .9$), pulse rate (OR, 1.00; 95% CI, 1.00-1.00; $P = .3$), ETCO$_2$ (OR, 1.00; 95% CI, 1.00-1.01; $P = .7$), use of dexmedetomidine (OR, 0.92; 95% CI, 0.83-1.02; $P = .12$), and presence of a lesion on standard brain MRI (OR, 0.99; 95% CI, 0.89-1.10; $P = .8$).

3.6 | Influence of PLD on ASL-SR in dogs with normal brain MRI

In phase 3, after excluding pASL-U dogs, 38 dogs had normal brain MRI with an average ASL-SR of 94% (Tables 6 to 8). The highest

ASL-SR was obtained using a PLD of 1525 ms (97.4%, 37/38). This ASL-SR was not significantly higher than the ASL-SR obtained using a PLD of 1025 ms (89.5%, 34/38; $P = .36$) or 2025 ms (94.7%, 36/38; $P = 1$).

3.7 | Influence of PLD on ASL-SR in dogs with pathological brain MRI

In phase 3, after excluding pASL-U dogs, 33 dogs had pathological brain MRI. The highest ASL-SR was obtained using a PLD of 1525 and 2025 ms (81.8%, 27/33; Tables 7 and 8). These results were not significantly different than the ASL-SR obtained using a PLD of 1025 ms (66.7%, 22/33; $P = .56$; Table 6).

3.8 | Influence of body weight and age on optimal PLD in dogs with normal brain MRI

In phase 3, 37 dogs had normal brain MRI and a gASL pattern with at least 1 of the 3 tested PLDs. Optimal PLD was 1025 ms in 13/37 (35.1%) dogs with a median body weight of 8 kg (IQR, 5-18; 1.2-32), 1525 ms in 17/37 (45.9%) with a median weight of 21 kg (IQR, 14-32; 6.1-39), and 2025 ms in 7/37 (19%) with a median weight of 29 kg (IQR, 25.5-31.5; 21-44; Figure 3). The difference in weight distribution was significant between 1025 and 1525 ms (*P* = .01) and between 1025 and 2025 ms (*P* = .01), suggesting that weight is a crucial factor for optimizing PLD.

Median age relative to optimal PLD was 4 years (IQR, 2-7) at 1025 ms, 8 years (IQR, 4-11) at 1525 ms, and 6 years (IQR, 4.5-7.75) at 2025 ms (Figure 4). The difference in age distribution was statistically significant only between 1025 and 1525 ms (*P* = .03), suggesting that age is not a critical factor for optimizing PLD.

3.9 | Influence of body weight and age on optimal PLD in dogs with pathological brain MRI

In phase 3, 27 dogs had pathological brain MRI and a gASL pattern with at least 1 of the 3 tested PLDs. Optimal PLD was 1025 ms in

7/27 dogs with a median body weight of 5 kg (IQR, 3.4-7), 1525 ms in 14/27 with a median weight of 12.8 kg (IQR, 12-21.5), and 2025 ms in 6/27 with a median weight of 31.5 kg (IQR, 25.3-34.8; Figure 5). As in dogs with normal brain MRI, weight appeared to be a critical factor for optimal PLD in dogs with abnormal MRI.

Median age relative to optimal PLD was 5 years (IQR, 4.3-8.5) at 1025 ms, 8.5 years (IQR, 7.1-10.9) at 1525 ms, and 9.5 years (IQR, 9-11.5) at 2025 ms (Figure 6). As in dogs with normal brain MRI, age did not appear as a critical factor for optimal PLD in dogs with abnormal brain MRI.

3.10 | Optimal PLD in dogs according to body weight

In all dogs of phase 3 excluding pASL-U dogs, multivariate analysis for the different PLDs in 3 groups of weight (<7 , 6-39, and >38 kg) showed that dogs weighing <7 kg (11/64) were significantly associated with an optimal PLD of 1025 ms (OR, 1.77; 95% CI, 1.37-2.29; *P* < .001), dogs weighing between 6 and 39 kg (53/64) were significantly associated with an optimal PLD of 1525 ms (OR, 1.58; 95% CI, 1.16-2.15; *P* = .005), and dogs weighing >38 kg (3/64) were significantly associated with an optimal PLD of 2025 ms (OR, 2.38; 95% CI, 1.39-4.09; *P* = .003).
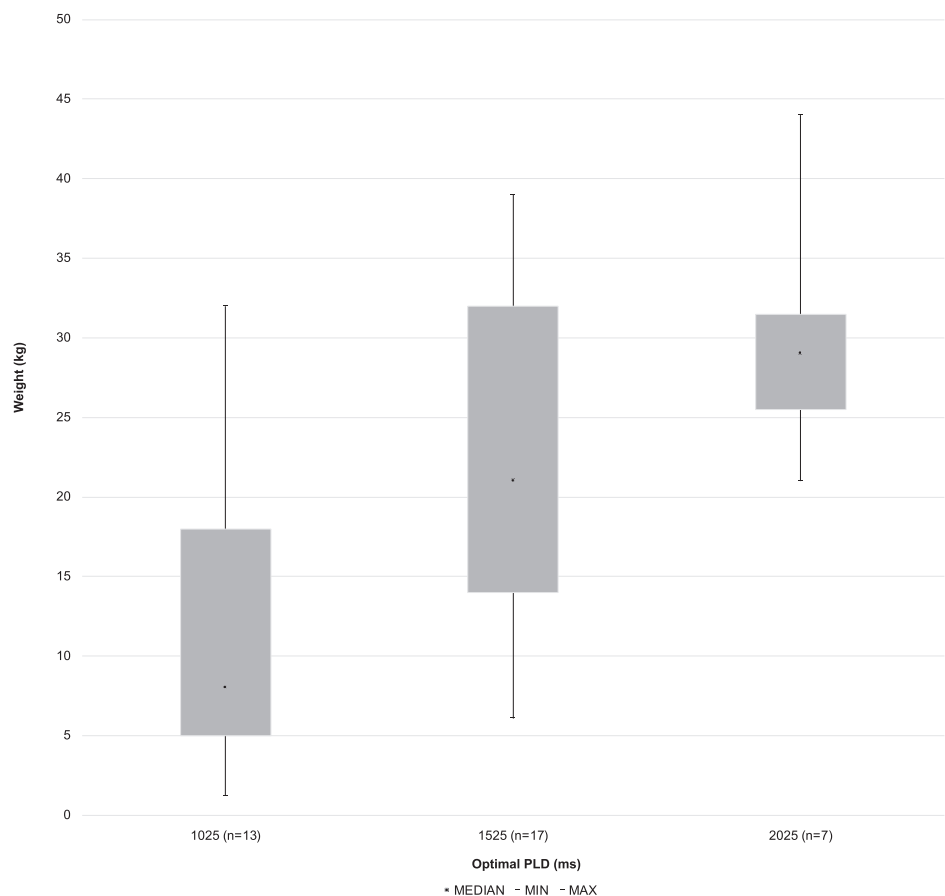

FIGURE 3 Box plot showing weight distribution relative to optimal PLD in 37 dogs with normal brain MRI. Optimal postlabeling delay (PLD) was determined in dogs of phase 3 that had normal brain magnetic resonance imaging (MRI) and gASL pattern with at least 1 of the PLDs tested
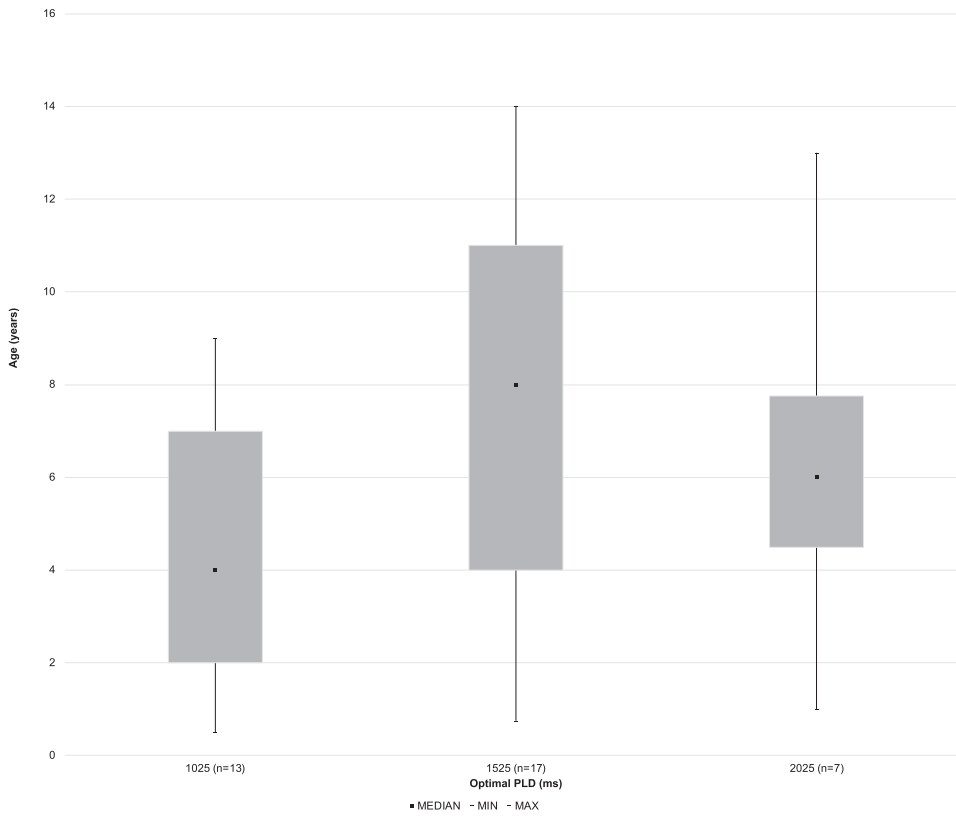
FIGURE 4 Box plot showing age distribution relative to optimal PLD in 37 dogs with normal brain MRI. Optimal postlabeling delay (PLD) was determined in dogs of phase 3 that had a normal brain magnetic resonance imaging (MRI) and a gASL pattern with at least 1 of the PLDs tested
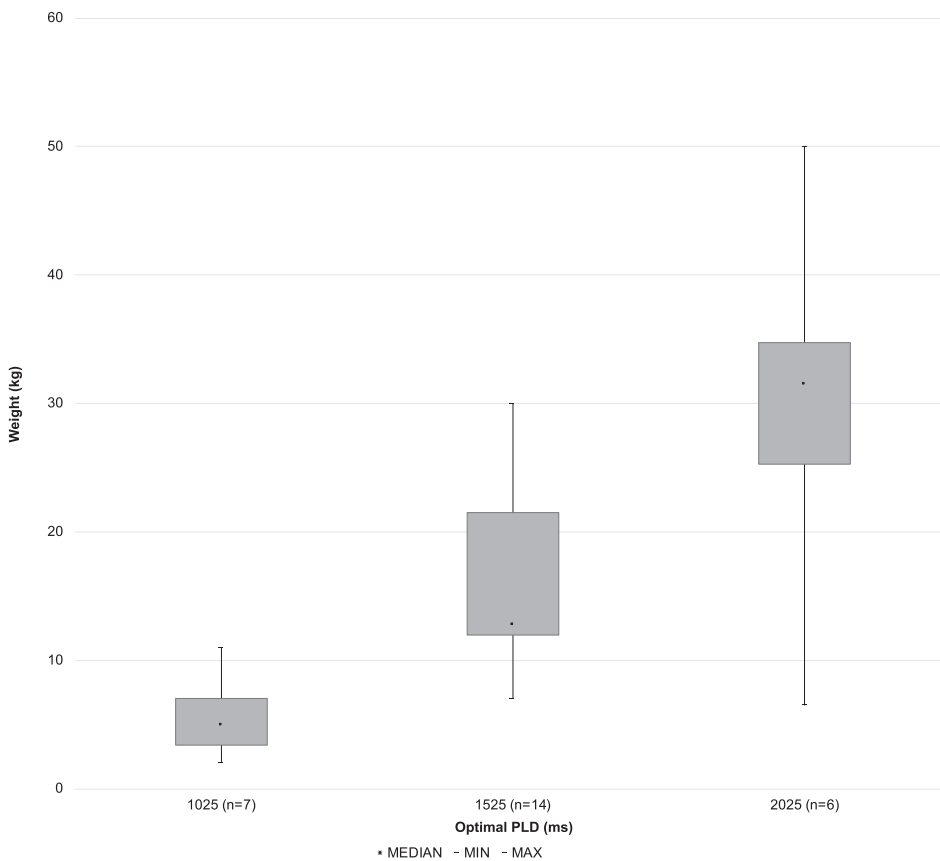

FIGURE 5 Box plot showing weight distribution relative to optimal PLD in 27 dogs with pathological brain MRI. Optimal postlabeling delay (PLD) was determined in dogs of phase 3 that had pathological brain magnetic resonance imaging (MRI) and gASL pattern with at least 1 of the PLDs tested
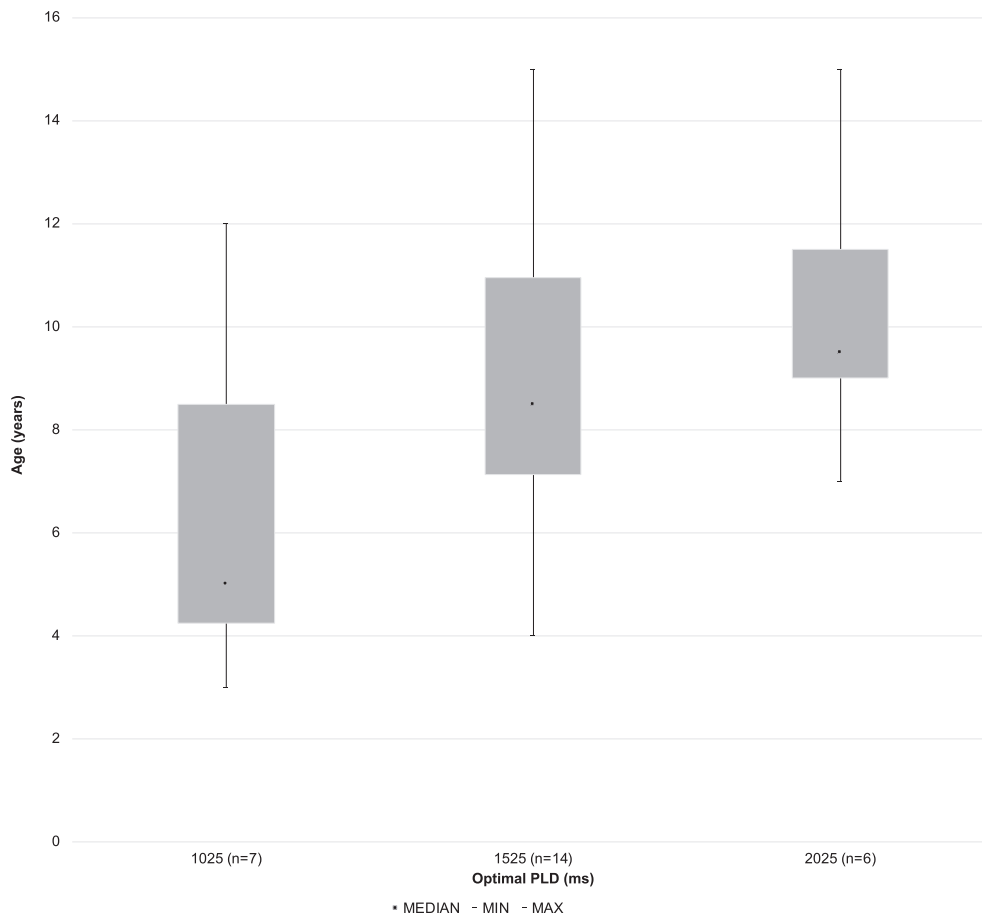
FIGURE 6 Box plot showing age distribution relative to optimal PLD in 27 dogs with pathological brain MRI. Optimal postlabeling delay (PLD) was determined in dogs of phase 3 that had pathological brain magnetic resonance imaging (MRI) and gASL pattern with at least 1 of the PLDs tested

3.11 | Poor quality ASL studies (pASL-B pattern) in dogs

In phase 3, 7 dogs showed a pASL-B pattern with each of the 3 tested PLDs, giving an ASL failure rate of 9.9% (7/71; Figure 2). All 7 dogs had high signal intensity in ECA branches, indicating proper tagging, and 6/7 had pathological brain MRI. The 7 dogs were compared with the 64 dogs of phase 3 that showed a gASL pattern with at least 1 PLD, using univariate and multivariate analyses. Results are presented in Supplemental Table 5 provided in Supporting Information 9. In both univariate and multivariate analyses, no significant difference was found between group pASL-B (7 dogs) and group gASL (64 dogs) for sex ratio (OR, 0.98; 95% CI, 0.84-1.14; $P = .8$), weight (OR, 1.00; 95% CI, 0.99-1.0; $P = .2$), dexmedetomidine use rate (OR, 1.07; 95% CI, 0.92-1.25; $P = .4$), ETCO$_2$ (OR, 1.01; 95% CI, 1.00-1.01; $P = .2$), and pulse rate (OR, 1.00; 95% CI, 1.00-1.00; $P = .9$). In univariate analysis, dogs in group pASL-B were significantly older than dogs in group gASL (median age, 11 years; IQR, 10.5-13.5 and 7.3 years; IQR, 4-9.3; $P = .02$). This result was confirmed by multivariate analysis (OR, 1.03; 95% CI, 1.01-1.05; $P = .01$).

In group pASL-B, final or presumed diagnoses included tumor (5/7), cerebellar ischemic stroke (1/7), and meningoencephalitis (1/7). The 5 tumors were thalamic glioma (n = 1), ventricular tumor (n = 3), and meningioma (n = 1). Four dogs in group pASL-B had a clinical evaluation compatible with intracranial hypertension and showed the following MRI findings: space-occupying lesion (4/4), mass effect (4/4), compression of an interventricular foramen (4/4), and brain herniation (1/4).

3.12 | Cerebral blood flow results in dogs with normal brain MRI

In phase 3, the 37 dogs with normal brain MRI that were selected for quantifying cortical CBF and thalamic CBF had a median age of 6 years (IQR, 3-9), median weight of 19 kg (IQR, 8-31), and sex ratio of 0.85 (M/F, 17/20). Table 9 presents the CBF results obtained in these dogs for each PLD and for the optimal PLD. Median optimal CBF was 114 mL/100 g/min (IQR, 94-132) in the cortex and 95 mL/100 g/min (IQR, 82-113) in the thalamic nuclei.

3.13 | Cerebral blood flow results in cats with normal brain MRI

Because of too few cats enrolled during phase 3, optimal PLD and optimal CBF were considered irrelevant in cats and are not presented here. Cortical and thalamic CBF were quantified in the 28 cats of group FM that had normal brain MRI using a PLD of 1025 ms. These cats had a median age of 8.5 years (IQR, 4-12), median weight of 4.7 kg (IQR, 4-5), and sex ratio of 1.2 (M/F, 15/13). Table 10 presents the cortical and thalamic CBF results obtained in

Anatomical region	PLD	n	CBF median (IQR)	CBF mean (SD)	CBF range
Cortex	1025 ms	34	97 (70-128)	105 (43.1)	44-217
	1525 ms	37	112 (89-129)	114 (45.6)	52-252
	2025 ms	36	103 (86-126)	107 (40.1)	46-247
	Optimal PLD	37	114 (94-132)	124 (48)	52-252
Thalamus	1025 ms	34	103 (86-122)	103 (30.1)	40-169
	1525 ms	37	99 (86-108)	94 (25)	47-165
	2025 ms	36	80 (69-91)	78 (17)	36-111
	Optimal PLD	37	95 (82-113)	101 (30)	47-165

TABLE 9 Cerebral blood flow (mL/100 g/min) measured in the cerebral cortex (gray matter) and thalamic nuclei (gray matter), in 37 dogs with normal standard brain MRI

Note: CBF was measured in dogs enrolled during phase 3 (FM slab position) that showed gASL pattern (good quality ASL) with at least 1 of the PLDs tested.
Abbreviations: CBF, cerebral blood flow; n, number of dogs; PLD, postlabeling delay.

TABLE 10 Cerebral blood flow (mL/100 g/min) measured in the cerebral cortex (gray matter) and thalamic nuclei (gray matter), in 28 cats with normal standard brain MRI, with PLD set at 1025 ms

Anatomical region	PLD	n	CBF median (IQR)	CBF mean (SD)	CBF range
Cortex	1025 ms	28	113 (94-150)	123 (42.1)	63-214
Thalamus	1025 ms	28	114 (94-141)	117 (33.5)	67-201

Note: CBF was measured in cats enrolled during phases 2 and 3 (FM slab position) that showed gASL pattern (good quality ASL) with PLD set at 1025 ms.
Abbreviations: CBF, cerebral blood flow; n, number of cats; PLD, postlabeling delay.

these cats. Median CBF was 113 mL/100 g/min in the cerebral cortex (IQR, 94-150) and 114 mL/100 g/min (IQR 94-141) in the thalamic nuclei.

4 | DISCUSSION

4.1 | Overall success rate of ASL in dogs and cats

In dogs, the highest ASL-SR was obtained by selecting a PLD of 1525 ms and an FM imaging slab position in both normal and pathological brain MRI dogs, and was 97.4% (37/38) and 81.8% (27/33), respectively (Tables 4-8). In cats, the highest relevant ASL-SR was obtained by selecting a PLD of 1025 ms and an FM imaging slab position in both normal and pathological brain MRI cats, and was 96.6% (28/29) and 80% (8/10), respectively (Tables 4-8). These findings substantiate the feasibility of brain ASL-MRI in dogs and cats at 1.5 T and the ability of ASL to evaluate cerebral perfusion.

4.2 | Labeling failure artifact

A pASL-U pattern always was associated with a signal defect in the ipsilateral ECA branches and represents a labeling failure artifact related to a cervical microchip with a lateral/ventrolateral position and a chip-to-FM distance <6 cm. A detailed discussion of the results, including the influence of species on the appearance of this artifact, is provided in Supporting Information 10.

4.3 | Optimal positioning of the imaging slab

The imaging slab position was an important quality factor of ASL as indicated by the significant near doubling of the ASL-SR (82.4% vs 47.7%) when the caudal border of the imaging slab was placed caudal to the cerebellum (FM position) rather than over the mid-length of the 2nd cervical vertebra (mid-C2 position; Supplemental Table 3 provided in Supporting information 7). Additionally, multivariate analysis showed that the FM position was significantly more frequent in gASL animals (80%, 169/210) than in pASL-B animals (43.8%, 35/80). These findings confirmed the crucial role of slab position in ASL success and lead to the recommendation of the FM position for implementing ASL-MRI in dogs and cats (Supplemental Table 4 provided in Supporting information 8). The PLD gives the labeled blood time to travel from the labeling site to the target imaging region, this time being referred to as the arterial transit time (ATT).[29] If the ATT is longer than the PLD, brain perfusion signal can be weak because labeled blood has not yet reached the brain capillary bed when ASL images are acquired, leading to an underestimation of CBF.[29,30,38] The dramatic increase in the ASL-SR is most likely because of a decrease in ATT when the labeling plane was displaced cranially from the mid-C2 position to the FM position. In humans, a method using anatomical landmarks consisting of the placement of the labeling plane just below the inferior border of the cerebellum ensures labeling of the posterior cerebral circulation.[7,8]

4.4 | Optimal PLD in dogs and recommended PLD in cats

In humans, PLD is 1 of the most important parameters for the ASL perfusion technique.[7,30] Its value directly determines the accuracy of the quantified CBF and should be adapted to the patient's conditions.[13,31,39,40]

A significant increase in weight was observed with increasing optimal PLD in dogs with or without a brain MRI lesion, suggesting that the heavier the dog, the higher the optimal PLD value. In humans, the optimal PLD is highly dependent on the presumed blood velocity.[8,15,30] The younger the individual, the faster the blood flow, and an increase in the PLD value is recommended with increasing age of the patients.[29,38,40] The increase in optimal PLD value with increasing weight in dogs could translate into a negative correlation between blood velocity and size or conformation with a lower arterial blood velocity and longer ATT in larger dogs and a higher flow velocity and shorter ATT in smaller dogs.

The multivariate analysis performed in phase 3 dogs showed a significant association between weight <7 kg and an optimal PLD of 1025 ms, weight between 6 and 39 kg and an optimal PLD of 1525 ms, and weight >38 kg and an optimal PLD of 2025 ms. Between 6 and 39 kg, overlaps of the weight ranges for the 3 optimal PLDs were observed (Figures 3 and 5). These overlaps may reflect the influence of additional variables recognized as factors influencing ATT in humans, including blood T1 relaxation (tracer half-life), cardiac output, and proximal vessel occlusion.[7,15,30,31] Within the limits of these results, the best agreement is to recommend a PLD of 1025 ms in dogs weighing <7 kg, a PLD of 2025 ms in dogs weighing >38 kg, and a PLD of 1525 ms for dogs between these weights. Considering that size, conformation, and weight in cats are much less variable than in dogs and that cats commonly weigh less than 7 kg, our findings in dogs suggest that 1025 ms could be a reasonable PLD to recommend in cats. This recommendation is reinforced by the ASL-SR obtained in cats with normal brain MRI at a PLD of 1025 ms (96.6%, 28/29).

In our study, age did not clearly emerge as a variable influencing optimal PLD in dogs. In humans, the well-documented positive correlation between age and PLD is illustrated by the progressive increase in PLD from 1025 ms in children to 3025 ms in elderly people.[19-26,38-42] Our findings suggest that age might not influence arterial blood velocity and ATT in dogs as it does in humans. The absence of documented spontaneous carotid atherosclerosis in dogs, in contrast to humans, might be a factor limiting the influence of age on ATT.

4.5 | Arterial spin labeling failure

In 7/71 dogs (9.9%), the quality of ASL images was poor despite optimal imaging slab positioning (FM position), absence of labeling failure (signal present in the ECA branches), and use of 3 different PLDs. In 4 dogs, MRI anomalies and clinical evaluation were compatible with intracranial hypertension. The absence of ASL brain perfusion signal in these dogs could be explained by their condition because intracranial hypertension may compromise CBF and alter brain perfusion because of cerebrospinal fluid flow disturbances and secondary brain edema.[43-45] In the remaining dogs (3/7), brain lesions were unlikely to cause intracranial hypertension. These 3 dogs were the oldest of group pASL-B (between 12 and 16 years). The 7 pASL-B dogs were significantly older than the 64 control g-ASL dogs in both univariate and multivariate analyses (Supplemented Table 5 provided in Supporting information 9). These findings are consistent with the negative relationship found between age and brain perfusion in dogs that most likely reflects a decrease in number, size, and function of neurons as a normal aging process.[46]

4.6 | Quantitative measurements of CBF in dogs and cats with a normal brain MRI

In our study, absolute CBF was quantitatively measured in dogs and cats using ASL-MRI at 1.5 T. Compared to dynamic susceptibility contrast-MRI in dogs,[34,35] ASL-MRI provided a quantitative measurement of CBF more easily (single drawing per ROI), more rapidly (no arterial input function required, no repeated ROI drawings over time), and noninvasively (no IV injection of an exogenous agent).

In 37 dogs with normal brain MRI, the median optimal CBF was 114 mL/100 g/min (IQR, 94-132) in the cortex and 95 mL/100 g/min (IQR, 82-113) in the thalamic nuclei (Table 9).

In 28 cats with normal brain MRI, the median CBF obtained with PLD set at 1025 ms was 113 mL/100 g/min in the cerebral cortex (IQR, 94-150) and 114 mL/100 g/min (IQR, 94-141) in the thalamic nuclei (Table 10). To our knowledge, these results are the first quantitative measurements of CBF published in cats in a clinical setting.

4.7 | Limitations

Our study had several limitations. The fixed time frame for data collection (16 months) with the prospective study design resulted in a very small number of cats in phase 3 (n = 7, after removal of cats displaying a microchip-related artifact) which precluded identification of optimal PLD in this species.

A variable influence of anesthesia on ASL quality and CBF was prevented by using the same anesthesia protocol in all 314 animals (induction with propofol and maintenance with isoflurane and oxygen). However, premedication, based on the individual's physical status, varied among animals. In humans, several studies have concluded that premedication had no effect on the regional distribution of CBF.[47-50] We therefore hypothesized that premedication would have minimal impact on ASL quality and CBF.

One of the main limitations of our study was the high number of analyses that were performed and the absence of any a priori correction for multiple analyses and inflated type 1 error. We tried to compensate for this weakness by performing multivariate analyses.

The last relevant limitation relates to the main inclusion criteria, which implied that selected animals were suspected of having a neurological disorder and could not be regarded as healthy although they had a normal standard brain MRI. A prospective study conducted on healthy dogs and cats would be valuable to confirm our results.

5 | CONCLUSION

Our prospective study is the first large-scale survey on brain perfusion ASL-MRI in dogs and cats demonstrating that ASL can be implemented at 1.5 Tesla with a relevant success rate in these species. A labeling failure artifact related to the cervical microchip can be observed. Recommendations for implementing ASL include (a) positioning of the imaging slab at the level of FM and (b) selection of the following PLDs: 1025 ms in all cats and in dogs <7 kg, 1525 ms in dogs between 7 and 38 kg, and 2025 ms in dogs >38 kg. Resting CBF measurements using ASL-MRI can be obtained easily within a few minutes in dogs and cats. Associated with anatomical and diffusion-weighted MRI sequences, ASL could be of critical importance in the diagnosis of many neurological disorders in dogs and cats and could be included in routine brain MRI protocols.

CONFLICT OF INTEREST DECLARATION
Authors declare no conflict of interest.

OFF-LABEL ANTIMICROBIAL DECLARATION
Authors declare no off-label use of antimicrobials.

INSTITUTIONAL ANIMAL CARE AND USE COMMITTEE (IACUC) OR OTHER APPROVAL DECLARATION
Approved by the Ethics Committee Jacques Bonnod of VetAgro Sup, registered #18 by the French Ministry of Research and Education.

HUMAN ETHICS APPROVAL DECLARATION
Authors declare human ethics approval was not needed for this study.

ORCID
Hugues Gaillot https://orcid.org/0000-0003-0804-1774

REFERENCES
1. Krainik A, Villien M, Troprès I, et al. Functional imaging of cerebral perfusion. *Diagn Interv Imaging*. 2013;94(12):1259-1278. https://doi.org/10.1016/j.diii.2013.08.004.
2. Zhang X, Li C-X. Arterial spin labeling perfusion magnetic resonance imaging of non-human primates. *Quant Imaging Med Surg*. 2016;6(5):573-581. https://doi.org/10.21037/qims.2016.10.05.
3. Buck J, Larkin JR, Simard MA, Khrapitchev AA, Chappell MA, Sibson NR. Sensitivity of multiphase pseudocontinuous arterial spin labelling (MP pCASL) magnetic resonance imaging for measuring brain and tumour blood flow in mice. *Contrast Media Mol Imaging*. 2018;7:ID4580919. https://doi.org/10.1155/2018/4580919.
4. Silva AC, Kim SG, Garwood M. Imaging blood flow in brain tumors using arterial spin labeling. *Magn Reson Med*. 2000;44(2):169-173. https://doi.org/10.1002/1522-2594(200008)44:2%3C169::AID-MRM1%3E3.0.CO;2-U.
5. Hendrich KS, Kochanek PM, Melick JA, et al. Cerebral perfusion during anesthesia with fentanyl, isoflurane, or pentobarbital in Normal rats studied by arterial spin-labeled MRI. *Magn Reson Med*. 2001;46(1):202-206. https://doi.org/10.1002/mrm.1178.
6. Grand S, Tahon F, Attye A, Lefournier V, le Bas JF, Krainik A. Perfusion imaging in brain disease. *Diagn Interv Imaging*. 2013;94(12):1241-1257. https://doi.org/10.1016/j.diii.2013.06.009.
7. Grade M, Hernandez Tamames JA, Pizzini FB, Achten E, Golay X, Smits M. A neuroradiologist's guide to arterial spin labeling MRI in clinical practice. *Neuroradiology*. 2015;57(12):1181-1202.
8. Alsop DC, Detre JA, Golay X, et al. Recommended implementation of arterial spin-labeled perfusion MRI for clinical applications: a consensus of the ISMRM Perfusion Study Group and the European Consortium for ASL in Dementia. *Magn Reson Med*. 2015;73(1):102-116. https://doi.org/10.1002/mrm.25197.
9. Wintermark MD, Sesay M, Barbier E, et al. Comparative overview of brain perfusion imaging techniques. *Stroke*. 2005;36:e83-e99. https://doi.org/10.1161/01.STR.0000177884.72657.8b.
10. Essig M, Shiroishi MS, Nguyen TB, et al. Perfusion MRI: the five most frequently asked technical questions. *Am J Roentgenol*. 2013;200(1):24-34.
11. Golay X, Petersen ET. Arterial spin labeling: benefits and pitfalls of high magnetic field. *Neuroimaging Clin N Am*. 2006;16(2):259-268. https://doi.org/10.1016/j.nic.2006.02.003.
12. Drazanova E, Ruda-Kucerova J, Kratka L, et al. Different effects of prenatal MAM vs. perinatal THC exposure on regional cerebral blood perfusion detected by arterial spin labelling MRI in rats. *Sci Rep*. 2019;9:6062.
13. Buxton RB, Franck LR, Wrong EC, et al. A general kinetic model for quantitative perfusion imaging with arterial spin labeling. *Magn Reson Med*. 1998;40(3):383-396. https://doi.org/10.1002/mrm.1910400308.
14. Deibler AR, Pollock JM, Kraft RA, Tan H, Burdette JH, Maldjian JA. Arterial spin-labeling in routine clinical practice, part 1: technique and artifacts. *Am J Neuroradiol*. 2008;29(7):1228-1234. https://doi.org/10.3174/ajnr.A1030.
15. Deibler AR, Pollock JM, Kraft RA, Tan H, Burdette JH, Maldjian JA. Arterial spin-labeling in routine clinical practice, part 2: hypoperfusion patterns. *Am J Neuroradiol*. 2008;29(7):1235-1241. https://doi.org/10.3174/ajnr.A1033.
16. Deibler AR, Pollock JM, Kraft RA, Tan H, Burdette JH, Maldjian JA. Arterial spin-labeling in routine clinical practice, part 3: hyperperfusion patterns. *Am J Neuroradiol*. 2008;29(8):1428-1435. https://doi.org/10.3174/ajnr.A1034.
17. Van Osch MJP, Teeuwisse WM, van Walderveen MAA, et al. Can arterial spin labeling detect white matter perfusion signal? *Magn Reson Med*. 2009;62(1):165-173. https://doi.org/10.1002/mrm.22002.
18. Ferré J-C, Bannier E, Raoult H, Mineur G, Carsin-Nicol B, Gauvrit JY. Arterial spin labeling (ASL) perfusion: techniques and clinical use. *Diagn Interv Imaging*. 2013;94(12):1211-1223.
19. Blauwblomme T, Boddaert N, Chémaly N, et al. Arterial spin labeling MRI: a step forward in non-invasive delineation of focal cortical dysplasia in children. *Epilepsy Res*. 2014;108(10):1932-1939. https://doi.org/10.1016/j.eplepsyres.2014.09.029.
20. Blauwblomme T, Naggara O, Brunelle F, et al. Arterial spin labeling magnetic resonance imaging: toward noninvasive diagnosis and follow-up of pediatric brain arteriovenous malformations. *J Neurosurg Pediatr*. 2015;15(4):451-448. https://doi.org/10.3171/2014.9.PEDS14194.
21. Blauwblomme T, Lemaitre H, Naggara O, et al. Cerebral blood flow improvement after indirect revascularization for pediatric Moyamoya disease: a statistical analysis of arterial spin-labeling MRI. *Am J Neuroradiol*. 2016;37(4):706-712.
22. Majer M, Mejdoubi M, Schertz M, Colombani S, Arrigo A. Raw arterial spin labeling data can help identify arterial occlusion in acute ischemic stroke. *Stroke*. 2015;46(6):e141-e144. https://doi.org/10.1161/STROKEAHA.114.008496.
23. Boulouis G, Shotard E, Dangouloff-Ros V, et al. Magnetic resonance imaging arterial-spin-labelling perfusion alterations in childhood

migraine with atypical aura: a case-control study. *Dev Med Child Neurol*. 2016;58(9):965-969. https://doi.org/10.1111/dmcn.13123.

24. Boulouis G, Dangouloff-Ros V, Boccara O, et al. Arterial spin-labeling to discriminate pediatric cervicofacial soft-tissue vascular anomalies. *Am J Neuroradiol*. 2017;38(3):633-638. https://doi.org/10.3174/ajnr.A5065.

25. Dangouloff-Ross V, Grevent D, Pagès M, et al. Choroid plexus neoplasms: toward a distinction between carcinoma and papilloma using arterial spin-labeling. *Am J Neuroradiol*. 2015;36(9):1786-1790. https://doi.org/10.3174/ajnr.A4332.

26. Dangouloff-Ross V, Deroulers C, Foissac F, et al. Arterial spin labeling to predict brain tumor grading in children: correlations between histopathologic vascular density and perfusion MR imaging. *Radiology*. 2016;281(2):553-566. https://doi.org/10.1148/radiol.2016152228.

27. Denis J, Dangouloff-Ross V, Graziella P, et al. Arterial spin labeling and central precocious puberty. *Clin Neuroradiol*. 2018;30(1):137-144. https://doi.org/10.1007/s00062-018-0738-5.

28. Saitovitch A, Lemaitre H, Rechtman E, et al. Neural and behavioral signature of human social perception. *Sci Rep*. 2019;9:9252. https://doi.org/10.1038/s41598-019-44977-8.

29. Woods JG, Chappell MA, Okell TW. A general framework for optimizing arterial spin labeling MRI experiments. *Magn Reson Med*. 2019;81(4):2474-2488. https://doi.org/10.1002/mrm.27580.

30. Mohindra N, Neyaz Z. Cerebral blood flow measurement with arterial spin labeling MRI: an underutilized technique. *Neurol India*. 2019;63(3):834-836.

31. Petcharunpaisan S, Ramalho J, Castillo M. Arterial spin labeling in neuroimaging. *World J Radiol*. 2010;2(10):384-398. https://doi.org/10.4329/wjr.v2.i10.384.

32. Zhao Q, Lee S, Kent M, et al. Dynamic contrast-enhanced magnetic resonance imaging of canine brain tumors. *Vet Radiol Ultrasound*. 2010;51(2):122-129. https://doi.org/10.1111/j.1740-8261.2009.01635.x.

33. Tidwell AS, Robertson ID. Magnetic resonance imaging of normal and abnormal brain perfusion. *Vet Radiol Ultrasound*. 2011;52(1):S62-S71. https://doi.org/10.1111/j.1740-8261.2010.01786.x.

34. Hartmann A, Driesen A, Lautenschläger IE, Scholz VB, Schmidt MJ. Quantitative analysis of brain perfusion in healthy dogs by means of magnetic resonance imaging. *Am J Vet Res*. 2016;77(11):1227-1235. https://doi.org/10.2460/ajvr.77.11.1227.

35. Stadler KL, Pease AP, Ballegeer EA. Dynamic susceptibility contrast magnetic resonance imaging protocol of the normal canine brain. *Front Vet Sci*. 2017;4:41. https://doi.org/10.3389/fvets.2017.00041.

36. McConnell JF. Ischemic brain disease and vascular anomalies. In: Mai W, ed. *Diagnostic MRI in Dogs and Cats*. Boca Raton, FL: Taylor & Francis Group; 2018:251-281.

37. Alisauskaite N, Wang-Leandro A, Dennler M, et al. Conventional and functional magnetic resonance imaging features of late subacute cortical laminar necrosis in a dog. *J Vet Intern Med*. 2019;33:1759-1765. https://doi.org/10.1111/jvim.15526.

38. Hu Y, Li Q, Li C, et al. Multidelay arterial spin-labeled perfusion magnetic resonance imaging in healthy individuals: a single-center experience. *Neurol India*. 2019;67(3):829-833.

39. Tang S, Liu X, He L, Liu B, Qin B, Feng C. Application of a 3D pseudocontinuous arterial spin-labeled perfusion MRI scan combined with a post-labeling delay value in the diagnosis of neonatal hypoxic-ischemic encephalopathy. *PLoS One*. 2019;14(7):e0219284. https://doi.org/10.1371/journal.pone.0219284.

40. Wang J-N, Li J, Liu H-J, et al. Application value of three-dimensional arterial spin labeling perfusion imaging in investigating cerebral blood flow dynamic in normal full-term neonates. *BMC Pediatr*. 2019;13(1):495. https://doi.org/10.1186/s12887-019-1876-x.

41. Teune LK, Renken RJ, de Jong BM, et al. Parkinson's disease-related perfusion and glucose metabolic brain patterns identified with PCASL-MRI and FDG-PET imaging. *Neuroimage Clin*. 2014;5:240-244. https://doi.org/10.1016/j.nicl.2014.06.007.

42. Boisgontier J, Tacchella JM, Lemaître H, et al. Anatomical and functional abnormalities on MRI in kabuki syndrome. *Neuroimage Clin*. 2019;21:101610. https://doi.org/10.1016/j.nicl.2018.11.020.

43. Kjällquist A, Siesjö BK, Zwetnow N. Effects of increased intracranial pressure on cerebral blood flow and on verebral venous pO$_2$, pCO$_2$, pH, lactate and pyruvate in dogs. *Acta Physiol Scand*. 1969;75(3):267-275. https://doi.org/10.1111/j.1748-1716.1969.tb04380.x.

44. Hekmatpanah J. Cerebral circulation and perfusion in experimental increased intracranial pressure. *J Neurosurg*. 1970;32(1):21-29.

45. Zhang X, Medow JE, Iskandar BJ. Invasive and noninvasive means of measuring intracranial pressure: a review. *Physiol Meas*. 2017;38(8):R143-R182.

46. Peremans K, Audenaert K, Blmanckaert P, et al. Effects of aging on brain perfusion and serotonin-2A receptor binding in the normal canine brain measured with single photon emission tomography. *Prog Neuropsychopharmacol Biol Psychiatry*. 2002;26(7–8):1393-1404. https://doi.org/10.1016/S0278-5846(02)00306-8.

47. Greicius MD, Kiviniemi V, Tervonen O, et al. Persistent default-mode network connectivity during light sedation. *Hum Brain Mapp*. 2008;29:838-847. https://doi.org/10.1002/hbm.20537.

48. Difrancesco MW, Rovertson SA, Karunanayaka P, et al. Bold fMRI in infants under sedation: comparing the impact of pentonarbital and propofol on auditory and language activation. *J Magn Reson Imaging*. 2013;38(5):1184-1195.

49. Veselis RA. Propofol and thiopental do not interfere with regional cerebral blood flow response at sedative concentrations. *Anesthesiology*. 2005;102:26-34.

50. Carsin-Vu A, Corouge I, Commowick O, et al. Measurement of pediatric regional cerebral blood flow from 6 months to 15 years of age in a clinical population. *Eur J Radiol*. 2018;101:38-44.

SUPPORTING INFORMATION

Additional supporting information may be found online in the Supporting Information section at the end of this article.